Supplementary Information

Defect repairment for enhanced piezo-phototronic MoS_2 flexible phototransistor

Pei Lin[a, b], Laipan Zhu[b, c], Ding Li[b, c], and Zhong Lin Wang[b, c, d,*]

[a] *Key Laboratory of Material Physics of Ministry of Education, School of Physics and Engineering, Zhengzhou University, Zhengzhou 450001, P. R. China*

[b] *CAS Center for Excellence in Nanoscience, Beijing Key Laboratory of Micro-nano Energy and Sensor, Beijing Institute of Nanoenergy and Nanosystems, Chinese Academy of Sciences, Beijing 100083, P. R. China*

[c] *School of Nanoscience and Technology, University of Chinese Academy of Sciences, Beijing 100049, P. R. China*

[d] *School of Material Science and Engineering, Georgia Institute of Technology, Atlanta, Georgia 30332, United States*

E-mail: zhong.wang@mse.gatech.edu

Supplementary note 1: CVD synthesis of MoS_2 and Raman characterization

The MoO_3 (Sigma-Aldrich, 99.97%) and sulfur (Sigma-Aldrich, 99.998%) powder were used as precursor for the CVD synthesis of MoS_2. Quartz boat containing MoO_3 (50 mg) was positioned in the center of tube furnace and SiO_2/Si substrate was placed face down above it, the excess sulfur powder was located in upstream of MoO_3. Then the temperature of MoO_3 was increased up to 850°C, and simultaneously the sulfur was heated to 180°C using heating strips. A mixture of Ar (500 sccm) and oxygen (2 sccm) flow was used as carrier gas, the whole growth process was carried out for 30 min. It is worth noting that the cool-down process of samples was conducted in sulfur vapor environment to deliberately introduce sulfur cluster on MoS_2 surface, which will facilitate the following self-healing of sulfur vacancy with poly(4-styrenesulfonate).[1] The synthetic MoS_2 flakes possess typical triangular shape with the length of triangle side several tens micrometers, as shown in Fig. S1a.

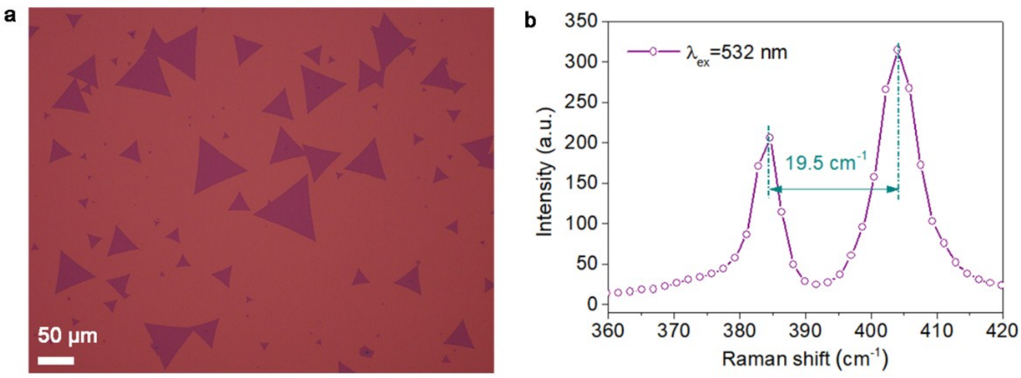

Fig. S1 (a) Optical microscopy image of synthetic MoS_2 flakes on SiO_2 substrate. (b) Raman spectra of the MoS_2 stimulated with 532 nm laser. The frequency separation of in-plane E1 2g and out-of-plane A_{1g} vibration mode is ~19.5 cm^{-1}, suggesting its monolayer nature.

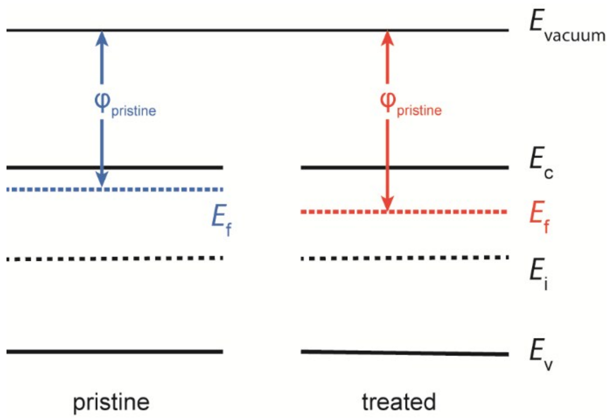

Fig. S2 Schematic Fermi level change of as-grown and treated MoS_2. The contact potential difference (CPD) between AFM tip and sample surface is defined as $V_{CPD}= (\varphi_{tip}-\varphi_{sample})/q$, where φ_{tip} and φ_{sample} represent the work function of AFM tip and MoS_2, respectively. From line profile in Figure 2d, the measured CPD decreases by ~50 meV after treatment, which indicates the increase of work function and Fermi level (E_f) of MoS_2 shifts toward intrinsic Fermi level (E_i).

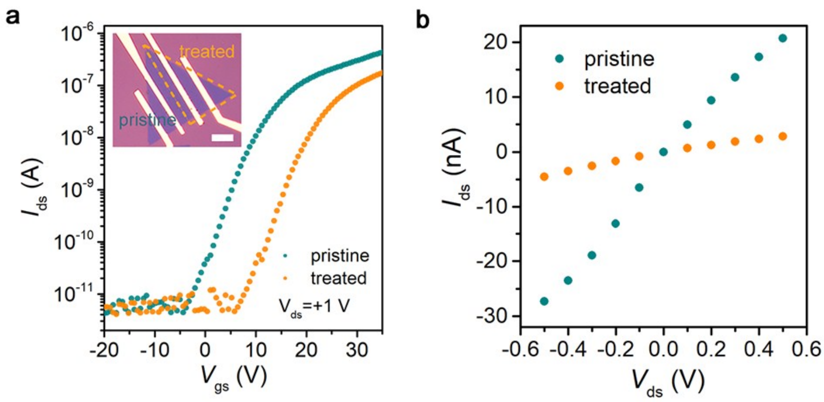

Fig. S3 (a) Typical I_{ds}-V_{gs} charactersitics of the pristine and locally-treated MoS_2 monolayer. (b) I_{ds}-V_{ds} characteristics of the pristine and locally-treated MoS_2 at zero gate voltage. The transistor channel can be approximately regarded as a resistor with conductivity $\sigma=q\mu N_D$, where μ and N_D represent field-effect mobility and MoS_2 electron concentration, respectively. The mobility can be extracted from I_{ds}-V_{gs} characteristics using the expression $\mu=[dI_{ds}/dV_{gs}]\times[L/(WC_iV_{ds})]$, where L and W is the channel length and width, C_i is the capacitance between the channel and back gate per unit area (SiO_2 thickness 300 nm).

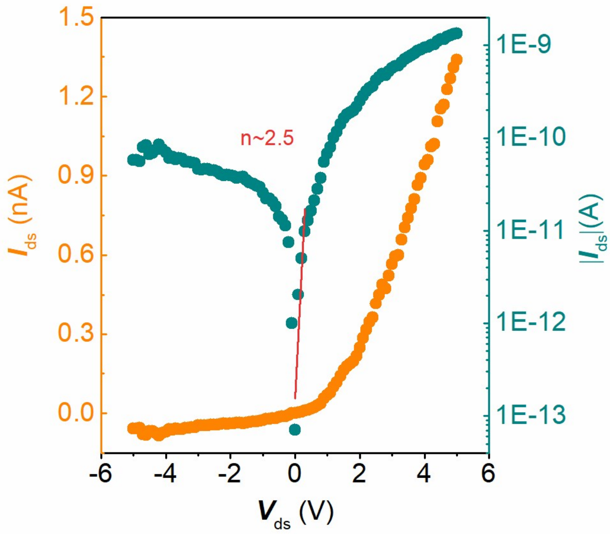

Fig. S4 Typical I_{ds}-V_{ds} curve of the two-terminal flexible device fabricated with monolayer MoS_2. A strong rectifying characteristic could be observed, suggesting the formation of Schottky barrier at Pd-MoS_2 interface and Cr-MoS_2 Ohmic contact.[2] The calculated ideality factor of Schottky contact is ~2.5 and the ON/OFF ratio is ~23 at ±5 V applied voltage.

Supplementary note 2: Experiment setup for characterizing piezo-phototronic process and calculation of applied strain

The piezo-phototronic process in our fabricated devices is characterized by measuring photoresponse under controlled illumination power and mechanical strain. Fig. S4a is photograph of the corresponding experiment setup. The 532 nm laser was illuminated over MoS_2 through focused optical fiber (spot diameter ~300 μm). The illumination intensity could be controlled by modulating the laser output power and attenuator. Meanwhile, the height between objective lens and sample was kept constant during the measurement process. The mechanical strain was applied with a self-made two-point bending apparatus, as shown in Fig. S4b. Due to the substantially smaller dimension of MoS_2 than PET, bending of substrate induces pure tensile/compressive strain in MoS_2 and the value can be estimated by $\varepsilon = d\sin\theta/2a$, where d represents thickness of PET, θ is the angle at the minimum strain point and 2a is separation of the bent PET.[3]

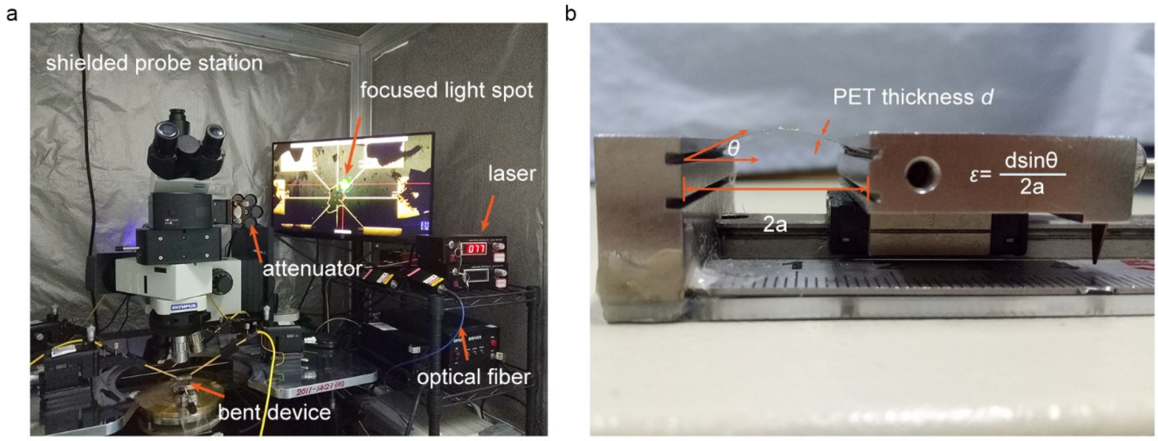

Fig. S5 (a) Photograph of the experiment setup for characterizing piezo-phototronic process in fabricated devices. (b) Photograph of the two-point bending apparatus for imposing mechanical strain on MoS_2 monolayer.

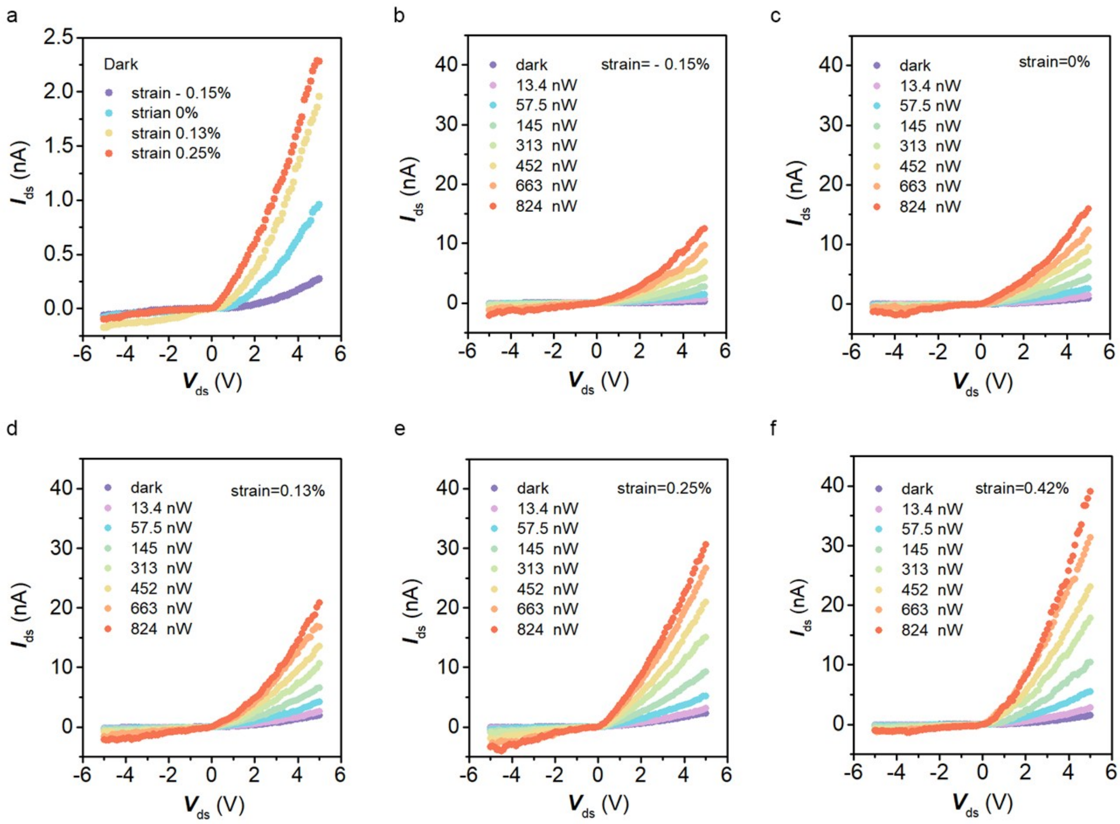

Fig. S6 (a) Strain dependency of dark current in fabricated devices with as-grown MoS_2, indicating the effective modulation of contact property with mechanical strain. (b-f) Photoresponse property of the devices under different applied static strains.

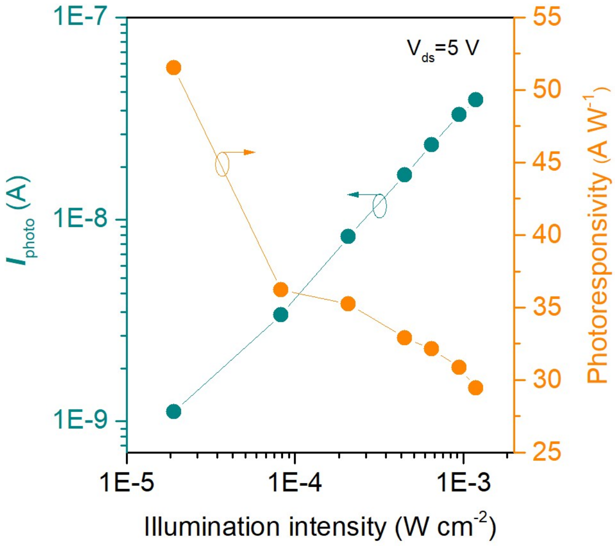

Fig. S7 The photoresponse and responsivity of fabricated device after MoS_2 being treated. The photocurrent shows a good linearity with optical power intensity in the whole measured range and responsivity is ~51.5 A W^{-1} at a low illumination intensity of 19.1 μW cm^{-2}.

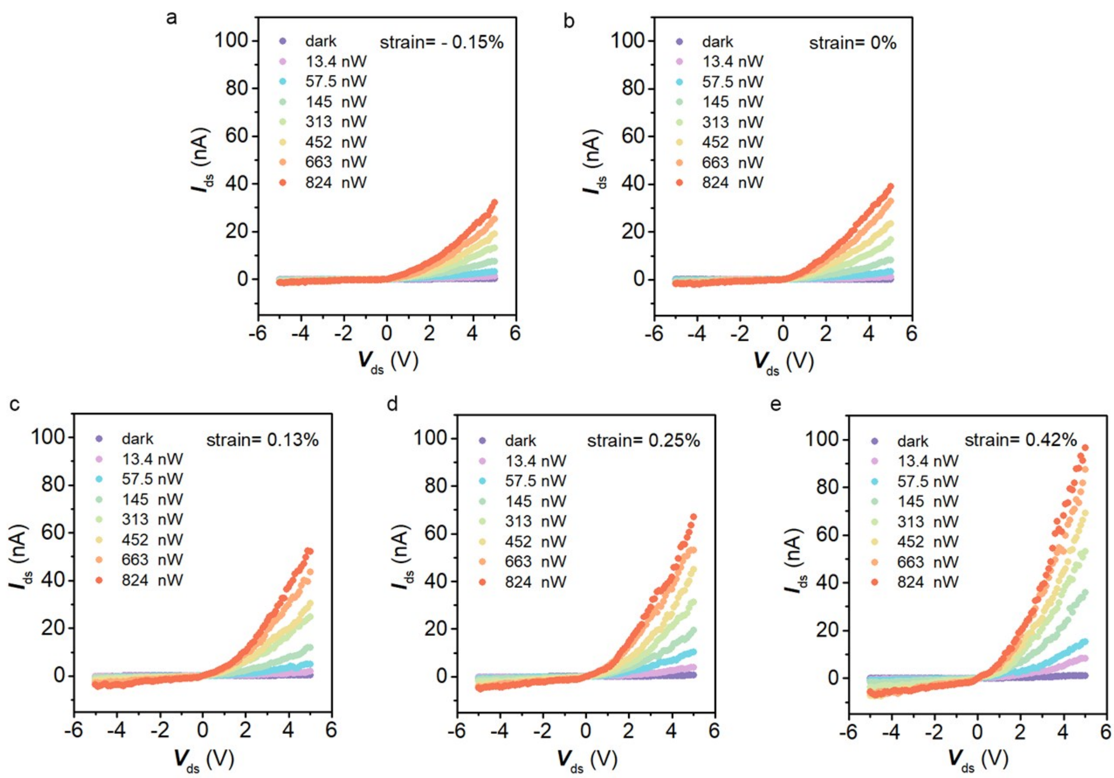

Fig. S8 Photoresponse curves of the treated MoS_2 monolayer flexible photodetector under different applied static strains.

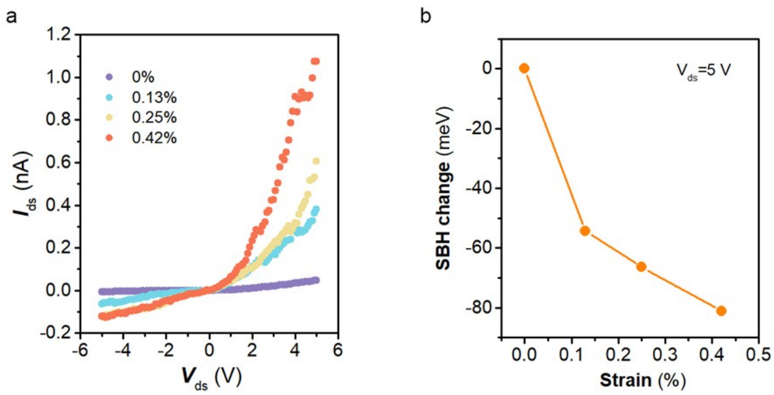

Fig. S9 (a) Electrical transport change of the treated MoS_2 device in dark, indicating strong strain dependency of interface contact property. (b) Calculated Schottky barrier height (SBH) change according to the thermionic emission theory for different applied strains.[4]

Supporting references

1. X. Zhang, Q. Liao, Z. Kang, B. Liu, Y. Ou, J. Du, J. Xiao, L. Gao, H. Shan, Y. Luo, Z. Fang, P. Wang, Z. Sun, Z. Zhang and Y. Zhang, *ACS Nano*, 2019, **13**, 3280-3291.

2. N. Kaushik, A. Nipane, F. Basheer, S. Dubey, S. Grover, M. M. Deshmukh and S. Lodha, *Appl. Phys. Lett.*, 2014, **105**, 113505.

3. S. B. Desai, G. Seol, J. S. Kang, H. Fang, C. Battaglia, R. Kapadia, J. W. Ager, J. Guo and A. Javey, *Nano Lett.*, 2014, **14**, 4592-4597.

4. J. Guo, R. Wen, J. Zhai and Z. L. Wang, *Sci. Bull.*, 2019, **64**, 128-135.